Joint Radar and Communication with 5G Signal: Algorithms, Prototypes and Experiments

Xiaojuan Zhang, Yonghong Zeng, Wenjiang Wang, Boon Shyang Lim
Institute for Infocomm Research, A*STAR, Singapore 138632
Email:{xzhang, yhzeng, wenjiang, bslim}@i2r.a-star.edu.sg

***Abstract*—We propose a joint radar and communication (JRC) system with 5G signal. Tailored radar sensing algorithms are proposed to detect the range, speed, and/or angle of the targets with the standardized 5G signals. A novel interference cancellation is developed to mitigate the self-interference in JRC. Furthermore, methods are proposed to detect human vital sign (breathing rate and heartbeat) after the target detection. A software defined radio (SDR) based prototype is built for the JRC system. We present experimental results demonstrating the prototype's capabilities in range, speed, and vital sign detection for both human and moving robot scenarios. These results underscore the platform's versatile sensing and communication capabilities. The SDR based design makes the prototype easy adaptable to various JRC algorithms and waveforms for different applications.**

I. Introduction

In Nov. 2023, ITU formally included the integrated sensing and communication (ISAC) in its IMT-2030 framework. The concept of Joint Radar and Communication (JRC) is one type of ISAC that uses shared hardware and waveforms to perform both sensing and communication tasks efficiently. This approach offers potential savings in spectrum utilization, power consumption, and overall costs, with wide-ranging benefits across various application domains, including assisted or automated driving systems [1] - [3].

Numerous algorithms for JRC have been proposed in the literature. Reference [4] provides comprehensive reviews, focusing on orthogonal frequency division multiplexing (OFDM) and multi-tone waveforms. Reference [5] proposes radar detection and estimation algorithms for cyclic prefixed OFDM (CP-OFDM), employing channel estimation and block processing tailored to CP-OFDM's structure. Reference [6] utilizes an autocorrelation-based approach for radar detection and estimation, leveraging the autocorrelation properties of preamble sequences in IEEE 802.11ad waveform. In our previous work [7] [8], we explored block-based waveforms with CP for JRC, including cyclic prefixed single carrier (CP-SC), OFDM, and their variants. We developed efficient, maximum likelihood (ML) principle-based algorithms for range and speed detection and estimation using these waveforms.

The 5G communication network is available everywhere and anytime, offering great potential for providing ubiquitous sensing. Thus, we propose a JRC system utilizing 5G signals. Tailored radar sensing algorithms are introduced to detect the range, speed, and/or angle of targets using standardized 5G signals. A novel interference cancellation technique is developed to mitigate self-interference in JRC. Furthermore, methods are proposed to detect human vital signs (breathing rate and heartbeat) following target detection.

However, many theoretical models rely on assumptions that may not hold in real-world environments, where challenges such as noise, interference, and hardware limitations can impact performance. There is a notable gap in the literature regarding experimental studies on JRC, particularly in the millimeter-wave (mmWave) spectrum. To address this, we developed a JRC prototype to evaluate the practical performance of these algorithms. Experimental results are provided to demonstrate the prototype's capabilities in range, speed, and vital sign detection for both human and moving robot scenarios. The prototype and experimental results are crucial for validating theoretical models, understanding environmental factors, addressing hardware constraints, refining algorithms, validating applications, ensuring regulatory compliance, and assessing commercial viability.

The remainder of this paper is organized as follows: Section II describes the system model. Sections III and IV detail the range and speed detection, and vital sign detection algorithms implemented on the developed JRC prototype, respectively. Section V outlines the hardware setup and presents experimental results. Finally, Section VI provides concluding remarks.

II. System Model

Fig. 1 depicts the system model for the JRC system. This setup comprises a transmitter (TX) that generates a communication signal following the standard 5G new radio (NR) protocol, which is then transmitted to targets via a TX antenna (ANT). An innovative feature of this system is its ability to embed modulated data in the transmitted signal, allowing the communication receiver (RX) to acquire communication data while radar receiver simultaneously performing radar sensing. By capturing and analyzing reflected signals from radar targets, the radar receiver can estimate both the range (distance) and speed of the targets. For human targets, the system can additionally estimate their breathing rate and heartbeat. While Fig. 1 illustrates two targets for clarity, real-world scenarios often involve multiple targets. Radar sensing can detect each target by distinguishing them based on distance and speed.

This research is supported by the National Research Foundation, Singapore and Infocomm Media Development Authority under its Future Communications Research Development Programme (Grant award number: FCP-ASTAR-TG-2022-003).

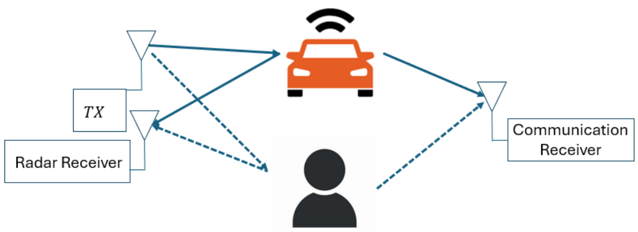

Fig. 1. Illustration of multi-target JRC system.

Let $s(t)$ be the transmitted baseband signal. The signal reflected from radar targets is received at the radar receiver. Assuming that there are L radar targets, the received baseband discrete signal is given by

$$y(nT_b) = \sum_{l=1}^{L} h_l s(nT_b - \tau_l) e^{j2\pi n\phi_l T_b} + w(nT_b) \quad (1)$$

where $h_l = \alpha_l e^{-j2\pi(f_c+\phi_l)\tau_l + j\omega + j\theta_l}$ is the complex channel gain of radar target l (random phase error is absorbed into this term as well), α_l is the attenuation coefficient of radar target l, f_c is the carrier frequency, $\phi_l = \frac{u_l}{c} f_c$ is the Doppler frequency shift induced by the moving of radar target l, u_l is the relative speed of radar target l , c is the speed of light, τ_l is the trip delay of radar target l, ω is the initial phase, θ_l is a phase error, T_b is the sampling period and $w(nT_b)$ is the noise term.

Radar receiver is to find the delay τ_l (corresponding to range) and Doppler shift ϕ_l (corresponding to the relative speed). Let $\varepsilon_l = \tau_l / T_b$, $v_l = \phi_l T_b$. Note that $\varepsilon_l = \tau_l / T_b$ may not be an integer. If so, we choose ε_l as the nearest integer to τ_l / T_b. To simplify notations, we denote $y(nT_b)$ by $y(n)$, $s(nT_b)$ by $s(n)$, and $w(nT_b)$ by $w(n)$, and will have

$$y(n) = \sum_{l=1}^{L} h_l s(n - \varepsilon_l)\ e^{j2\pi n v_l} + w(n), n = 0, 1, \ldots . \quad (2)$$

The 5G time domain signal $s(n)$ has a "block structure" and is composed of M blocks with each block having a length of $N_a = N + N_p$, where N is the length of data block and N_p is the length of CP. In each block, the first N_p symbols (the CP) are the repetition of the last N_p symbols. To cater for this structure, we divide the received discrete signal $y(n)$ into blocks of length N_a. In each block, the first N_p elements (corresponding to the CP of that block) are discarded. The block m (after discarding the CP) is denoted as $y_m(n), n = 0, 1, \ldots, N-1, m = 0, 1, \ldots,\ M-1$. Assuming that the normalized delay is always smaller than the CP length $\varepsilon_l \leq N_p$, the received signal can be expressed as

$$y_m(n) = \sum_{l=1}^{L} \hat{h}_l s_m\left(\langle n - \varepsilon_l \rangle_N\right) e^{j2\pi n v_l} e^{j2\pi m N_a v_l} + w_m(n) \quad (3)$$

where $\hat{h}_l = h_l e^{j2\pi N_p v_l}$ and $\langle n \rangle_K$ denotes the remainder of n modulo K: $\langle n \rangle_K = n \bmod K$.

III. Range and Speed Detections, and Interference Cancellations

In our previous work, we proposed the Fast Cyclic Correlation Radar (FCCR), which was derived from the maximum likelihood (ML) principle and can be used for any waveform with the CP structure [7]. Theoretically, it is nearly optimal given that the delay is within the CP range. Let the cyclic correlation of the received signal and the transmitted signal be

$$r\left(n, m\right) = \sum_{p=0}^{N-1} y_m(p) s_m^*\left(\langle p - n \rangle_N\right), n = 0, 1, \ldots, N-1. \quad (4)$$

Let the Discrete Fourier Transform (DFT) of $r\left(n, m\right)$ on the second dimension be

$$R\left(n, k\right) = \sum_{m=0}^{M-1} r\left(n, m\right) e^{j\frac{-2\pi mk}{M_1}} \quad (5)$$

where $M_1 = qM$ with q being a positive integer number. We call $R\left(n, k\right)$ the range-Doppler matrix (RDM). It is proved in [7] that the ML estimation for the range and speed can be very well approximated by the maximization below

$$(n_1,\ k_1) = \arg \max_{(n,\ \ k)} |R\left(n, k\right)|. \quad (6)$$

The normalized range and speed are then obtained as: $\varepsilon_1 = n_1$, and $v_1 = k_1 / (M_1 N_a)$.

In the developed JRC prototype, we utilize the NI Universal Software Radio Peripheral (USRP) for transmitting and receiving 5G signals. Due to the close proximity of the transmit and receive antennas, there is significant leakage of the transmit signal into the receive signal, leading to strong interference of the transmitted signal with the reflected signal. The power of this self-interference signal can overshadow that of the reflected signal, making radar targets undetectable. To mitigate this challenge, we propose a novel interference cancellation scheme to enhance radar target detection. In this context, the self-interference can be treated as a radar target with zero delay. Let $Q_m(n) = Y_m(n) S_m(n)^*$, where $Y_m(n)$ and $S_m(n)$ are the DFT of $y_m(n)$ and $s_m(n)$, respectively. By averaging $Q_m(n)$ across all data subcarriers, we can determine the contribution of the zero-delay radar target, which is self-interference. Consequently, we can cancel the self-interference as:

$$\tilde{Q}_m(n) = Q_m(n) - \frac{1}{|S_{data}|} \sum_{i \in S_{data}} Q_m(i) \quad (7)$$

where S_{data} is the set of data subcarriers and $|S_{data}|$ is the cardinality of S_{data}.

After this, we perform an Inverse Fast Fourier Transform (IFFT) on $\tilde{Q}_m(n)$ to obtain the correlation term $\tilde{r}(n, m)$ after cancelling self-interference. Finally, we perform a DFT on the updated correlation $\tilde{r}(n, m)$ along the second dimension to obtain the updated RDM. The peaks in the updated RDM will indicate the range and speed of the radar targets. This approach effectively mitigates the impact of self-interference, enabling accurate detection and estimation of radar targets even in challenging conditions with high levels of self-interference.

IV. BREATHING RATE AND HEARTBEAT DETECTION

When the target is a human, the JRC prototype can also detect breathing rate and heartbeat. Due to the slow movement of the chest wall during breathing and heartbeat, the delay ε_l remains relatively constant within a single radar detection interval. This stability does not affect the range and speed detection described previously, which only requires a single radar detection. However, for detecting breathing rate and heartbeat, multiple radar detections over time are necessary. Here, we refine the system model to incorporate the impact of breathing and heartbeat.

The transmitted 5G RF signal is represented as:

$$a(t) = \text{Re}\left\{s(t)e^{j2\pi f_c t}\right\} \tag{8}$$

where $s(t)$ is the baseband 5G signal and f_c is the center frequency.

When this signal $a(t)$ is reflected back by a human target with a time-varying chest-wall motion $x(t)$ at a distance r, the total distance traveled between the transmitter and receiver is $2r + 2x(t)$. The round-trip time is:

$$2d(t) = \frac{2r}{c} + \frac{2x(t)}{c} \tag{9}$$

where c is the speed of light.

Thus, the received signal at the radar receiver is

$$g(t) = h \cdot \text{Re}\left\{s(t - 2d(t))e^{j2\pi f_c(t-2d(t))}\right\} \tag{10}$$

where h is the complex channel gain.

The received signal is downconverted to baseband as

$$\tilde{g}(t) = h \cdot s(t - 2d(t))e^{-j4\pi f_c d(t)}. \tag{11}$$

Given the slow movement of the chest wall due to breathing and heartbeat, the delay ε_l remains approximately constant over a short radar detection interval. This allows us to focus on longer-term changes for vital sign detection. The updated system model considers the periodic chest-wall displacement caused by breathing and heartbeat, which modulates the reflected radar signal over multiple detection intervals. By continuously monitoring the phase and amplitude variations in the radar returns, we can extract the periodic components corresponding to breathing rate and heartbeat [9].

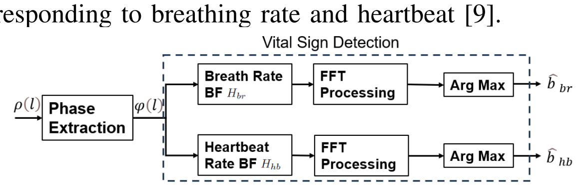

Fig. 2. Vital signs detection block.

Here's how the process unfolds as shown in Fig. 2.

- Collecting Multiple Radar Detections: We gather radar data over an extended period to capture the slow periodic movements of the chest wall. Let the radar detection interval be denoted as Δ, where Δ is the time for the data frame plus the idle time as shown in Fig. 3, and $l = 0, 1, \ldots, L_1 - 1$ be the index for the detection interval. The RDM at the l-th detection can be written as

$$\tilde{R}(n, k, l) = R(n, k)e^{-j2\pi f_c\left(\frac{2r}{c} + \frac{2x(l\Delta)}{c}\right)}. \tag{12}$$

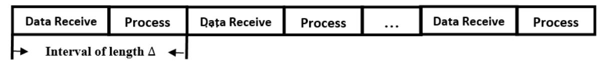

Fig. 3. Breathing and heartbeat rate detection with multiple sensing intervals.

- Analyzing Phase Variations: The phase variations in the radar signal are analyzed to detect the periodicity corresponding to breathing and heartbeat. We obtain the peaks for RDM of each radar detection, yielding

$$\rho(l) = \tilde{R}(\varepsilon_1, M_1 N_a v_1)e^{-j2\pi f_c\left(\frac{2r}{c} + \frac{2x(l\Delta)}{c}\right)}. \tag{13}$$

The phase of each peak $\rho(l)$ is

$$\phi(l) = -f_c\left(\frac{2r}{c} + \frac{2x(l\Delta)}{c}\right). \tag{14}$$

Thus, chest-wall displacement at the l-th detection is

$$x(l\Delta) = -\frac{c\phi(l)}{2f_c} - r. \tag{15}$$

Obviously, $\phi(l), l = 0, 1, \ldots, L_1 - 1$, can be used to estimate the frequency (change rate) of slow motion of chest $x(t)$, that is, the breathing and heartbeat rate.

- Signal Processing Techniques: Filtering and spectral analysis techniques are employed to isolate and identify the frequency components associated with breathing and heartbeat:

$$\hat{b}_{br} = \max_{k\in\{0,1,2,\ldots,L_1-1\}} \frac{1}{L_1}\sum_{l=0}^{L_1-1} H_{br}(\phi(l))e^{-\frac{j2\pi lk}{L_1}} \tag{16}$$

$$\hat{b}_{hb} = \max_{k\in\{0,1,2,\ldots,L_1-1\}} \frac{1}{L_1}\sum_{l=0}^{L_1-1} H_{hb}(\phi(l))e^{-\frac{j2\pi lk}{L_1}} \tag{17}$$

where H_{br} and H_{hb} are bandpass filters applied for breathing and heartbeat detection, respectively.

- Calculating Vital Signs: The breathing rate f_{br} and heartbeat rate f_{hb} are estimated as:

$$f_{br} = \hat{b}_{br} \cdot \frac{1}{L\Delta} \tag{18}$$

$$f_{hb} = \hat{b}_{hb} \cdot \frac{1}{L\Delta}. \tag{19}$$

V. PROTOTYPE SETUP AND EVALUATION RESULTS

Fig. 4 illustrates the block diagram of the developed JRC prototype, comprising two primary components: the USRP for transmitting and/or receiving 5G signals, and PCs for signal generation and post-processing. This setup facilitates integrated sensing and communication capabilities, including range, speed, and vital sign detection functionalities. In the configuration, the PC on the left side is responsible for radar detection after receiving the reflected signals passed by the USRP on the left side. Meanwhile, the PC on the right side performs data demodulation and decoding after obtaining the received signal passed by the USRP on the right side.

Fig. 5 depicts the hardware setup of the developed JRC prototype. The transmitted 5G signal is generated using the MATLAB 5G toolbox. We utilize the NI USRP2944 for both transmitting and receiving 5G signals. To handle the mmWave frequencies from 24 GHz to 44 GHz, the EVAL-ADMV1013 and EVAL-ADMV1014 evaluation boards are employed for up-converting sub-6 GHz signals to mmWave and vice versa.

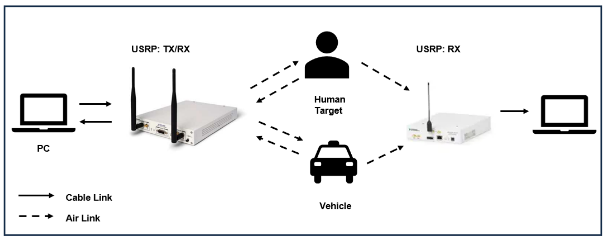

Fig. 4. JRC Prototype Block Diagram.

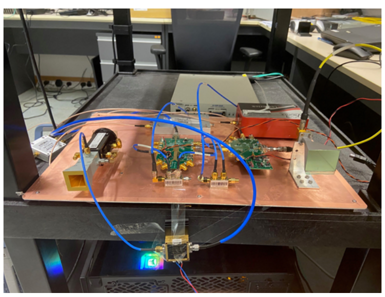

Fig. 5. Physical setup of mmWave JRC prototype.

Once the NI USRP receives the reflected signal from the radar targets, it forwards the signal to the radar detection module for further processing. While the results in this paper focus on experiments conducted with 5G signals, this platform is versatile enough to assess the performance of other signal types, such as Orthogonal Time Frequency Space (OTFS). To evaluate different signal types, we can generate the desired signals and input them into the USRP for processing.

It is important to note that while the results discussed here evaluate the performance of the range, speed, and vital sign detection algorithms described in Sections III and IV, the platform's flexibility allows for the evaluation of various other JRC algorithms. This can be achieved by replacing the radar detection module with alternative algorithms suited for specific applications or research purposes.

The parameters we use for evaluation are given in Table I. We use the communication receiver in the 5G toolbox for data demodulation and decoding, which achieves a bit error rate less than 10^{-6} at short distance around 5m. In the following, we will focus on the radar sensing performances.

We explore two scenarios in this study. In the first scenario, we focus on static targets, specifically a human seated approximately 1.2 meters away. Fig. 6 presents the results of range and speed detection. Since the person remains stationary, their speed is zero. This figure demonstrates that our developed JRC

TABLE I
EXPERIMENTS PARAMETERS

Channel bandwidth	100 MHz
Carrier frequency	40 GHz
Subcarrier spacing	30 kHz
Modulation scheme	QPSK
FFT size	4096
Symbols per slot	14
Slots per subframe	1
Slots per frame	20
LDPC code rate	490/1024
LDPC encoding algorithm	Normalized min-sum
Maximum LDPC iteration count	6
Number of transmit antennas	1
Number of receive antennas	1

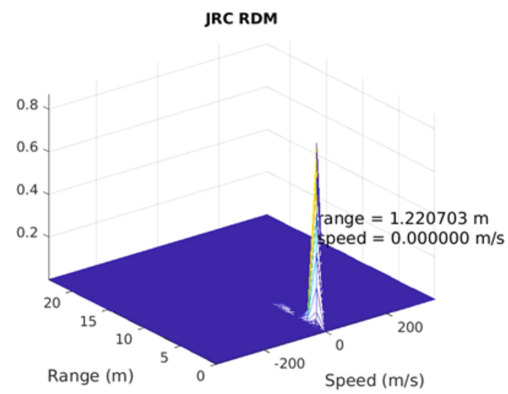

Fig. 6. Range and speed detection performance.

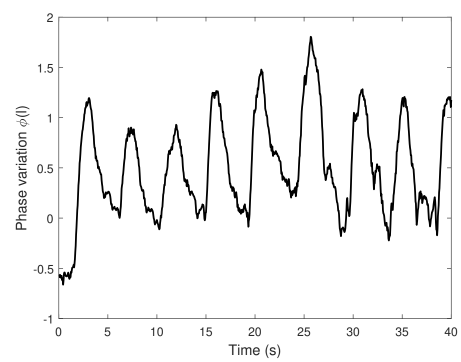

Fig. 7. Phase variation of peaks on RDM.

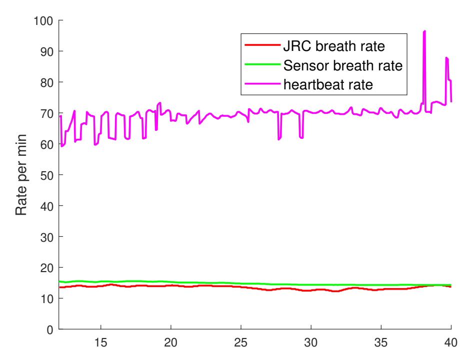

Fig. 8. Vital sign detection performance.

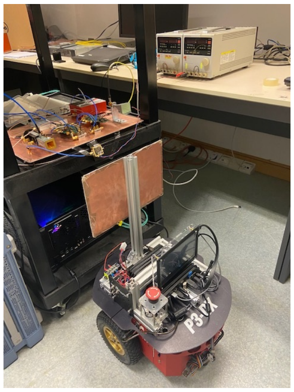

Fig. 9. Physical setup of robot speed detection.

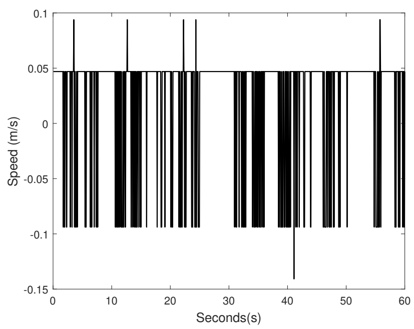

Fig. 10. Speed result of robot moving.

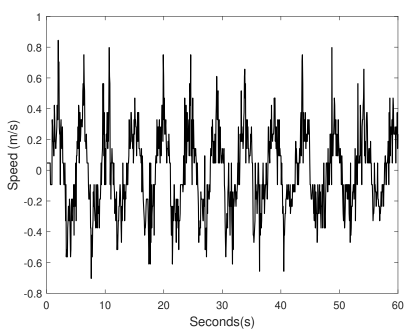

Fig. 11. Speed result of human moving.

prototype accurately detects both the range and speed of the radar target. Fig. 7 illustrates the phase variations of peaks in the RDM, collected at radar detection intervals of 0.04 seconds, which indicates the human chest movement with time including the human breathing and heartbeat information. To benchmark our vital sign detection, the person also wears the Respiration Sensor - SA9311M, which provides breathing rate information based on physical chest movements. Fig. 8 shows that the breathing rate detected by the JRC prototype closely matches the results obtained from the respiration sensor. However, the detection of heartbeat exhibits fluctuations due to various interfering frequencies. These interferences can originate from human movement, harmonics of breathing signals, or reflected interference from the surrounding environment. Increasing the frequency of mmWave signals could potentially amplify heartbeat signals, thereby enhancing detectability and result reliability.

In the second scenario, we investigate moving targets, where either a human or a robot moves back and forth in front of the prototype, as depicted in Fig. 9. Fig. 10 illustrates the speed results when a robot is in motion, with its speed controlled remotely to ensure slow and stable movement. Fig. 11 displays the speed detection results when a human moves. Due to the inability to control human speed, there is notable fluctuation in their movement speed. Note that the positive and negative speeds depicted in both figures correspond to the forward and backward movements of the targets.

VI. Conclusions

We have developed a JRC system and prototype based on 5G signal, with tailored radar sensing algorithms to detect the range, speed, and/or angle of the targets, a novel interference cancellation scheme to mitigate the self-interference, and practical methods to detect human vital sign (breathing rate and heartbeat) after the target detection. Experimental results were presented to demonstrate its sensing capabilities, encompassing range, speed, and vital sign detection. The prototype serves as a versatile platform for evaluating diverse JRC algorithms and waveforms, offering valuable insights for practical application development. Future work will focus on improving the sensing algorithms for multi-target detection, interference cancellation, and real-time implementation.

Acknowledgment

The authors would like to thank Dr. S. M. Sun for her guidance, and their colleagues C. M. Pang, X. M. Qing, Nasimuddin, A. Adiwahono, Varghese, C. K. Ang, and R. Jayabal for their help with the hardware setup. They also appreciate the discussions with colleagues F. Chin, Y. H. Wang, and Y. G. Ma, and extend their gratitude to student M. J. Xue for his assistance with the simulation platform.

References

[1] F. Liu, Y. Cui, J. Xu, T. X. Han, Y. C. Eldar and S. Buzzi, “Integrated sensing and communications: towards dual-functional wireless networks for 6G and beyond”, *IEEE Journal on Selected Areas in Communications*, vol. 40, issue 6, pp. 1728-1767, June 2022.

[2] J. A. Zhang, F. Liu, et al., “An overview of signal processing techniques for joint communication and radar sensing,” *IEEE Journal of Selected Topics in Signal Processing*, vol. 15, no. 6, pp. 1295-1315, Nov. 2021.

[3] 3GPP TR22.837, “Feasibility Study on Integrated Sensing and Communication”, V19.3.0, March 2024.

[4] L. Gaudio1, M. Kobayashi, B. Bissinger, and G. Caire, “Performance analysis of joint radar and communication using OFDM and OTFS”, *IEEE ICC Workshop*, 2019.

[5] M. Braun, C. Sturm, and F. K. Jondral, “Maximum likelihood speed and distance estimation for OFDM radar,” *in Proc. IEEE 2010 Radar Conf.*, Washington, DC, May 2010.

[6] P. Kumari, J. Choi, N. Gonzalez-Prelcic, and R. W. Heath Jr, “IEEE 802.11ad-based Radar: An Approach to Joint Vehicular Communication-Radar System,” *IEEE Trans. Vehicular Tech.*, vol. 67, no. 4, 2018.

[7] Y. H. Zeng, Y. G. Ma, and S. M. Sun, “Joint radar-communication with cyclic prefixed single carrier waveforms”, *IEEE Trans. Vehicular Tech.*, vol. 69, no. 4, pp. 4069-4079, 2020.

[8] X. J. Zhang, Y. G. Ma, Y. H. Zeng, S. M. Sun and Y. H. Wang, “Bistatic joint radar and communication with 5G signal for range speed angle detections”, IEEE VTC-fall, Oct. 2023.

[9] G. Paterniani, et al., “Radar-based monitoring of vital signs: a tutorial overview”, *Proceedings of the IEEE*, vol. 111, no. 3, pp. 277-317, 2023.